

# Analysis of the Single-FFT Receiver for Layered ACO-OFDM in Visible Light Communications

Xiaoshuang Liu , Jianfeng Li , Jianke Li , and Zhitong Huang 

**Abstract**—Layered asymmetrically clipped optical orthogonal frequency division multiplexing (LACO-OFDM) has a high spectral efficiency. However, an iterative detection with a pair of fast Fourier transform (FFT) and inverse fast Fourier transform (IFFT) is required for LACO-OFDM, which increases the complexity for the receiver of LACO-OFDM. In this paper, the performance of the receiver with a single FFT is analyzed for LACO-OFDM in visible light communications. In the single-FFT receiver, the different layers of ACO-OFDM signals are distinguished in time domain without the FFT/IFFT pair. Because only one FFT is employed in the proposed receiver, the complexity of  $O(M \log_2 N)$  can be achieved, which is much lower than the complexity of the conventional LACO-OFDM receiver. Simulation results illustrate that the proposed scheme has a signal-to-noise ratio (SNR) penalty of 1dB  $\sim$  3dB compared with the conventional solution in additive white Gaussian noise (AWGN) channel. However, the proposed receiver outperforms conventional LACO-OFDM solution in light emitting diode (LED) nonlinearity channel.

**Index Terms**—Intensity modulation with direct detection (IM/DD), Layered asymmetrically clipped optical orthogonal frequency division multiplexing (LACO-OFDM), modulation, optical communications, visible light communications.

## I. INTRODUCTION

OPTICAL orthogonal frequency division multiplexing (OFDM) is being considered as a candidate for visible light communications (VLC) because of many advantages such as high spectral efficiency and anti-multipath fading [1]–[4]. Asymmetrically clipped optical OFDM (ACO-OFDM) do not need any direct current (DC) bias, which is a power efficient OFDM technique for an intensity modulation/direct detection (IM/DD) system [5]. However, ACO-OFDM is not efficient in terms of bandwidth, in which only odd subcarriers are used

Manuscript received August 15, 2019; revised March 31, 2020 and May 7, 2020; accepted May 11, 2020. Date of publication May 14, 2020; date of current version September 1, 2020. This work was supported in part by National Natural Science Foundation of China under Grant 61801165, in part by Natural Science Foundation of Hebei Province under Grant F2017207006, in part by Research Fund of Hebei University of Economics and Business under Grants 2016KYQ02, 2019YB12, and in part by Science and Technology Project of Hebei Province (16960314D). (Corresponding author: Jianfeng Li)

Xiaoshuang Liu, Jianfeng Li, and Jianke Li are with the School of Information Technology, Hebei University of Economics and Business, Shijiazhuang 050061, China (e-mail: liuxiaoshuang@heuet.edu.cn; lijianfeng@heuet.edu.cn; lijianke@heuet.edu.cn).

Zhitong Huang is with the State Key Laboratory of Information Photonics and Optical Communications, Beijing University of Posts and Telecommunications, Beijing 100876, China (e-mail: hzt@bupt.edu.cn).

Color versions of one or more of the figures in this article are available online at <https://ieeexplore.ieee.org>.

Digital Object Identifier 10.1109/JLT.2020.2994633

to transmit information symbols. Recently, there are several schemes to improve the spectral efficiency for ACO-OFDM including asymmetrically clipped DC biased optical OFDM (ADO-OFDM) [6], hybrid ACO-OFDM (HACO-OFDM) [7], spectral and energy efficient OFDM (SEE-OFDM) [8], enhanced unipolar OFDM (eU-OFDM) [9], enhanced ACO-OFDM (eACO-OFDM) [10], augmented spectral efficiency discrete multi-tone (ASE-DMT) [11] and layered ACO-OFDM (LACO-OFDM) [12]. Compared with these schemes, LACO-OFDM needs the lowest signal-to-noise ratio (SNR) for a given spectral efficiency [13]. In LACO-OFDM systems, multiple ACO-OFDM layers could be transmitted simultaneously and a complicated iterative receiver with a pair of fast Fourier transform (FFT) and inverse fast Fourier transform (IFFT) is required to recover the each layer. An improved receiver is proposed for LACO-OFDM, which distinguishes different layers of ACO-OFDM signals in the time domain [14]. In [15], a diversity combining based receiver is utilized to improve the LACO-OFDM performance. A two-stage receiver is proposed, in which a soft interference cancellation module is used in [16]. Wang et al. experimentally show that LACO-OFDM exhibits its great potential in short-haul optical transmission link [17]. However, in all these schemes, the iterative detection with the FFT/IFFT pair is still required in the receiver, which increases the computational complexity for the receiver of LACO-OFDM.

High computational complexity of LACO-OFDM may restrict its application in VLC systems. A single-FFT transmitter has been shown in [17], by which the complexity of the transmitter can be reduced. However, the complexity of the receiver remains a challenge for LACO-OFDM. A single-FFT receiver using the symmetry properties of ACO-OFDM has been actually proposed for SEE-OFDM in [8]. Furthermore, in our previous work, we proposed a diversity combining scheme via symmetry recovering for ACO-OFDM systems [18]. Symmetry recovering is a simple signal processing in time domain without the FFT/IFFT pair which can reduce the computational complexity for the receiver, which may be a great benefit for LACO-OFDM.

In this paper, a low-complexity receiver with only single FFT for LACO-OFDM is proposed. We also compare the performance of the proposed scheme with the conventional technique in additive white Gaussian noise (AWGN) and light emitting diode (LED) nonlinearity channel. It is shown that compared with the conventional scheme, the proposed receiver is insensitive to the LED nonlinearity.

The rest of this paper is organized as follows. The single-FFT receiver is developed in Section II. Simulation results and

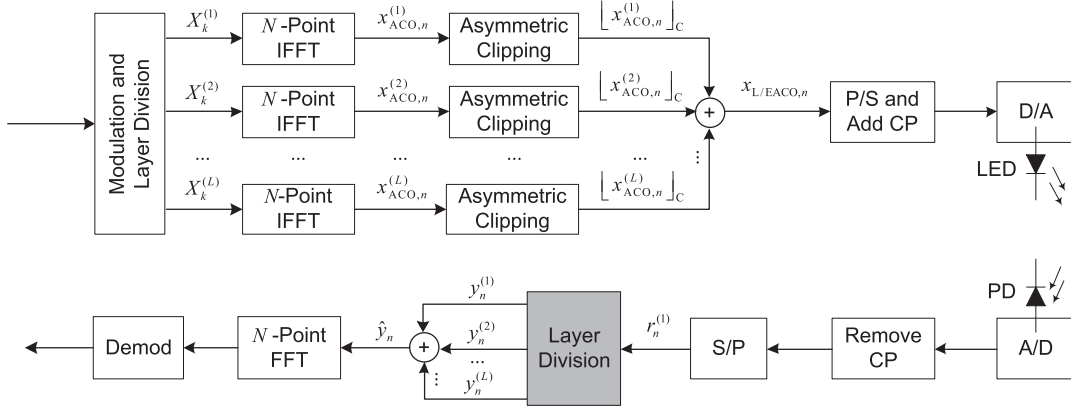


Fig. 1. Block diagram of single-FFT receiver for the LACO-OFDM based VLC system.

discussions are shown in Section III. Finally, conclusions are drawn in Section IV

## II. SYSTEM DESCRIPTION

A LACO-OFDM based VLC system with  $N$  subcarriers is shown in Fig. 1. In LACO-OFDM systems, multiple ACO-OFDM layers are transmitted in parallel to improve the spectral efficiency. Subcarriers in frequency domain are divided into subgroups which carry different layers [15]:

$$X_k^{(l)} = \begin{cases} X, & k \in K_{ACO}^l, \\ 0, & \text{otherwise,} \end{cases} \quad (1)$$

where  $X_k^{(l)}$  and  $K_{ACO}^l$  denote the frequency-domain signal of Layer  $l$  and the data-carrying subcarriers for Layer  $l$ .  $X_k^{(l)}$  has Hermitian symmetry:  $X_k^{(l)} = X_{N-k}^{(l)*}$ .  $K_{ACO}^l$  for Layer  $l$  can be written by [15]

$$K_{ACO}^l = \{1 \times 2^{l-1}, 3 \times 2^{l-1}, 5 \times 2^{l-1}, \dots, N - 2^{l-1}\}. \quad (2)$$

As shown in Fig. 1,  $N$ -point IFFTs are performed respectively for each layer. After IFFT the  $n^{\text{th}}$  time-domain sample of LACO-OFDM for Layer  $l$  is [12]

$$x_{ACO,n}^{(l)} = \frac{1}{\sqrt{N}} \sum_{k=0}^{N-1} X_k^{(l)} \exp\left(\frac{j2\pi nk}{N}\right), \quad n = 0, 1, \dots, N-1, \quad (3)$$

which has the anti-symmetry as

$$x_{ACO,n}^{(l)} = -x_{ACO,n+N/2^l}^{(l)}, \quad \text{mod}(n, N/2^{l-1}) < N/2^l, \quad (4)$$

for  $n = 0, 1, \dots, N - N/2^l - 1$ . For higher layers (Layer  $l > 1$ ), ACO-OFDM symbol also exhibits the symmetry property:

$$x_{ACO,n}^{(l+1)} = x_{ACO,n+N/2^l}^{(l+1)}, \quad \text{mod}(n, N/2^{l-1}) < N/2^l, \quad (5)$$

for  $n = 0, 1, \dots, N - N/2^l - 1$ . By reason of anti-symmetry, the negative parts of  $x_{ACO,n}^{(l)}$  can be clipped to generate a unipolar

signal:

$$\begin{aligned} \left[ x_{ACO,n}^{(l)} \right]_C &= \begin{cases} x_{ACO,n}^{(l)}, & x_{ACO,n}^{(l)} \geq 0 \\ 0, & x_{ACO,n}^{(l)} < 0 \end{cases} \\ &= \frac{1}{2} x_{ACO,n}^{(l)} + x_{\text{Clip},n}^{(l)}, \quad n = 0, 1, \dots, N-1, \end{aligned} \quad (6)$$

where  $x_{\text{Clip},n}^{(l)}$  is the clipping distortion that only fall on the clipping distortion-carrying subcarriers in frequency domain, which are denoted by

$$K_{\text{Clip}}^l = \{k - 2^{l-1} : k \in K_{ACO}^l\}. \quad (7)$$

It is noted that since  $x_{\text{Clip},n}^{(l)}$  in (6) is generated from the even subcarriers only, it has symmetry property in time domain: [6]

$$x_{\text{Clip},n}^{(l)} = x_{\text{Clip},n+N/2^l}^{(l)}, \quad \text{mod}(n, N/2^{l-1}) < N/2^l, \quad (8)$$

for  $n = 0, 1, \dots, N - N/2^l - 1$ . All layers of ACO-OFDM are then combined as

$$x_{L/EACO,n} = \sum_{l=1}^L \left[ x_{ACO,n}^{(l)} \right]_C, \quad n = 0, 1, \dots, N-1, \quad (9)$$

where  $L$  denotes the number of layers. The maximum value of  $L$  is equal to  $\log_2 N - 1$ . Then the LACO-OFDM signal is input to an LED to generate the optical signal after a digital to analog (D/A) converter and the cyclic prefix (CP) addition.

At the receiver in VLC systems, a photodiode (PD) is generally used to convert the received intensity of incident light into electrical signal, which is called IM/DD in optical transmission systems. The thermal noise and shot noise from the LED and PD in VLC systems are usually modeled as an AWGN channel [6]–[12], [19]. In addition, the LED nonlinear noise can't be ignored, which may limit the performance of VLC systems [20]. To simplify the derivation, AWGN channel is assumed in this section. We can have

$$\begin{aligned} r_n^{(1)} &= x_{L/EACO,n} + e_n \\ &= \sum_{l=1}^L \left( \frac{1}{2} x_{ACO,n}^{(l)} + x_{\text{Clip},n}^{(l)} \right) + e_n, \quad n = 0, 1, \dots, N-1, \end{aligned} \quad (10)$$

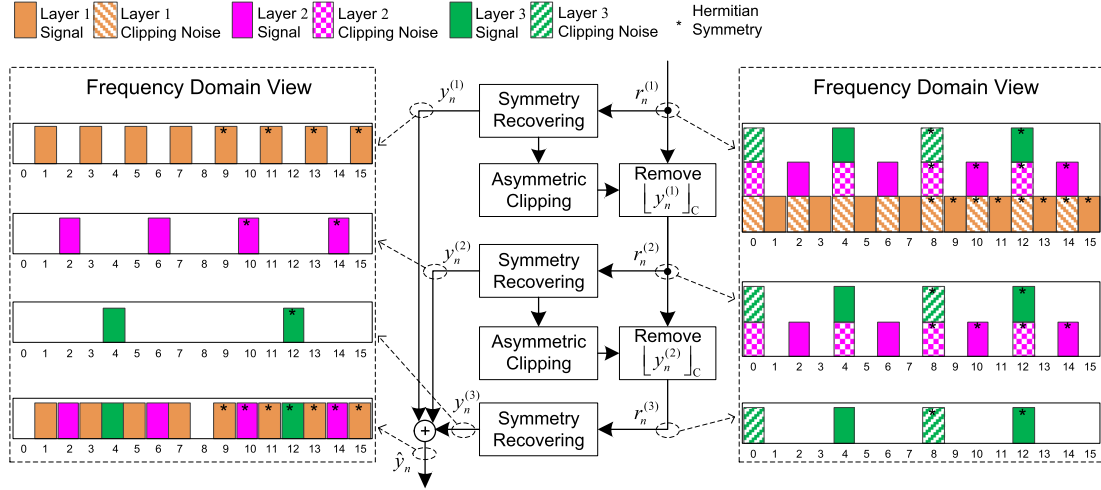


Fig. 2. Block diagram of the proposed layer division for LACO-OFDM with 16-FFT points and 3 layers.

where  $r_n^{(l)}$  is received signal with all layers superposed from Layer  $l$  to Layer  $L$  and  $e_n$  is the discrete time version of AWGN. According to (5), (8) and (10), we have

$$r_n^{(l+1)} \approx r_{n+N/2^l}^{(l+1)}, \quad \text{mod}(n, N/2^{l-1}) < N/2^l, \quad (11)$$

for  $n = 0, 1, \dots, N - N/2^l - 1$ . In LACO-OFDM systems, when the negative clipping distortion of lower layers has been removed, ACO-OFDM symbols of higher layers can be recovered [12]. Conventional LACO-OFDM systems could only rely on an iterative receiver, in which different layers are distinguished by the FFT/IFFT pair. In single-FFT receiver, different layers are distinguished by a layer division in time domain as shown in Fig. 1. According to (4),  $x_{\text{ACO},n}^{(l)}$  has the anti-symmetry. According to (8) and (11),  $x_{\text{Clip},n}^{(l)}$  and  $r_n^{(l+1)}$  follow the symmetry property respectively. Therefore, combining (4), (8), (10) and (11), we can obtain Layer  $l$  signal

$$y_n^{(l)} = x_{\text{ACO},n}^{(l)} + e_n^{(l)} = \begin{cases} \left( r_n^{(l)} - r_{n+N/2^l}^{(l)} \right), & \text{mod}(n, N/2^{l-1}) < N/2^l \\ \left( r_n^{(l)} - r_{n-N/2^l}^{(l)} \right), & \text{mod}(n, N/2^{l-1}) \geq N/2^l \end{cases}, \quad (12)$$

for  $n = 0, 1, \dots, N - N/2^l - 1$ , where  $e_n^{(l)}$  denote the AWGN for Layer  $l$ . Since  $x_{\text{ACO},n}^{(l)}$  follows anti-symmetry, the operation of (12) is called ‘‘symmetry recovering’’ [18]. Unlike in [8], in our scheme when the signal and the clipping distortion from the Layer 1 are entirely removed, Layer 2 can be recovered as shown in Fig. 2. Therefore, after Layer  $l$  signal  $y_n^{(l)}$  has been clipped, we can remove  $[y_n^{(l)}]_C$  from  $r_n^{(l)}$  to obtain the higher layer signal:

$$r_n^{(l+1)} = r_n^{(l)} - [y_n^{(l)}]_C, \quad n = 0, 1, \dots, N - 1. \quad (13)$$

The iteration loop of (12) and (13) is performed in the layer division until all layers have been recovered. To describe the layer division more intuitively, signal processing steps for

LACO-OFDM with 3 layers and 16 subcarriers are shown in Fig. 2. For the reason that subcarriers in different layers are orthogonal, all layers of ACO-OFDM could be combined by

$$\hat{y}_n = \sum_{l=1}^L y_n^{(l)}, \quad n = 0, 1, \dots, N - 1. \quad (14)$$

Owing to  $\hat{y}_n$  including all layers information, only one FFT is required to translate  $\hat{y}_n$  from time domain to frequency domain, then to be demodulated.

The complexity of the receiver is analyzed below. In the proposed receiver only one  $N$ -point FFT is employed and its computational complexity is  $O(N \log_2 N)$ . In the proposed layer division, several subtraction operations of  $N$ -point with the complexity of  $O(N)$  are required such as symmetry recovering and asymmetric clipping. There are  $L$  iterations of  $O(N)$  for symmetry recovering.  $L-1$  iterations of  $O(N)$  are required for asymmetric clipping. There are  $L-1$  iterations of  $O(N)$  for the loop of (13). Therefore, the complexity of the proposed receiver with  $L$  layers is given by

$$C_{\text{pro}} = O(N \log_2 N) + \sum_{l=1}^L O(N) + 2 \sum_{l=1}^{L-1} O(N) = O(N \log_2 N). \quad (15)$$

The complexity of the proposed receiver is  $O(N \log_2 N)$ .

In the conventional receiver in [12], besides an  $N$ -point FFT,  $L-1$  iterations of different sizes of FFT/IFFT pairs and asymmetric clipping are utilized in the iterative receiver. The complexity of the receiver is  $(5 - 1/2^{L-3})O(N \log_2(N))$ , which has been illustrated in detail in [12]. In another receiver in [13], [17], in addition to an  $N$ -point FFT,  $L-1$  iterations of  $N$ -point of FFT/IFFT pairs are required, which have the complexity of  $2 \sum_{l=1}^{L-1} O(N \log_2(N))$ .  $L-1$  iterations of  $O(N)$  are also required for asymmetric clipping. Therefore, the complexity of the receiver in [13], [17] with  $L$  layers can be written as

$$C = O(N \log_2 N) + 2 \sum_{l=1}^{L-1} O(N \log_2 N) + \sum_{l=1}^{L-1} O(N) = LO(N \log_2 N). \quad (16)$$

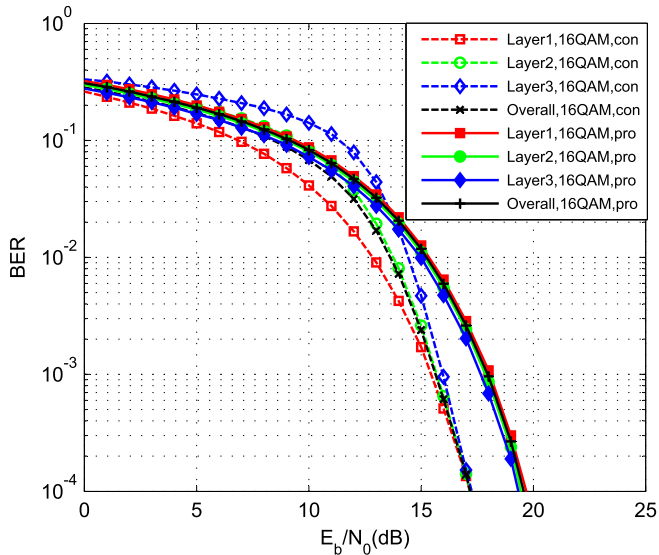


Fig. 3. BER performance of the proposed (pro) and the conventional (con) scheme with 3 layers and 16-QAM in AWGN channel.

### III. NUMERICAL RESULTS

We present Monte-Carlo simulation results in this section. The bit error ratio (BER) performance of the proposed scheme (pro) and conventional scheme (con) in [12] are evaluated by simulations in terms of the bit energy to noise power ratio  $E_b/N_0$ . The FFT/IFFT size of  $N = 1024$  is employed. The number of layers in LACO-OFDM is set to 2, 3 and 4. The subcarriers are modulated by different quadrature amplitude modulation (QAM) constellations of 4-QAM, 16-QAM, and 64-QAM. The BER performance of the proposed receiver is presented in an AWGN channel in section A. Furthermore, to depict the LED nonlinearity, the Rapps LED model is used in this section B.

#### A. AWGN Channel

Fig. 3 shows the performance of the proposed scheme and the conventional solution with 3 layers and 16-QAM in AWGN channel. In conventional LACO-OFDM systems, the same power of each modulated subcarrier is loaded on each layer. In the conventional receiver, an iterative detection (eq. (11) in [12]) in the iterative detection is utilized for the current layer before recovering the higher layer, which improves the estimation accuracy and reduces the BER for higher layers, and then to be a convergence for BER curves as shown in Fig. 3. In the proposed scheme, ACO-OFDM symbols of each layer are detected independently. For the same BER level of all layers in the proposed scheme, subcarrier power of Layer  $l$  is allocated by  $P_l$  that has  $4P_1 = 2P_2 = P_3$ , with which each layer can have the same power in time domain. There is a simple explanation as follow. The maximum number of data-carrying subcarriers of Layer 1 is  $m_1 = 512$ , where  $m_l$  is the number of data-carrying subcarriers of Layer  $l$ . The maximum number of data-carrying subcarriers of Layer 2 is  $m_2 = 256$ , which leads to a half power as much as Layer 1 for the signal in time domain. In addition, Layer 3 has  $m_3 = 128$  leading to a quarter of power as much

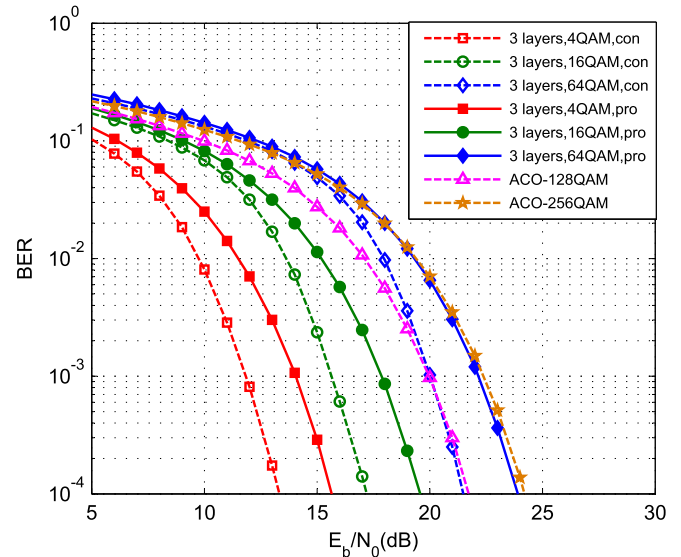


Fig. 4. BER performance comparison of the proposed and the conventional scheme with 3 layers and various types of  $M$ -QAM.

as Layer 1. If ACO-OFDM symbols of each layer are detected independently without the iterative detection, the lower power in time domain will lead to the worse BER for higher layers. However, without the iterative detection, the noise from the current layer may be added to higher layers. It is obvious that the BER performance of the proposed scheme is degraded by almost 2 dB compared with the conventional receiver as shown in Fig. 3.

Fig. 4 illustrates that the average BER performance of LACO-OFDM with 3 layers for various types of  $M$ -QAM. The performance of the proposed scheme is degraded by 2 dB at the BER of  $10^{-3}$  compared with the conventional scheme. It is due to the fact that each layer is detected independently without iterative detection for the proposed scheme. The LACO-OFDM spectral efficiencies of 3 layers are 0.875 bits/s/Hz (4-QAM), 1.75 bits/s/Hz (16-QAM) and 2.625 bits/s/Hz (64-QAM), where the length of CP is omitted as shown in [12]. The results of two kinds of original ACO-OFDM with 128-QAM (1.75 bits/s/Hz) and 256-QAM (2 bits/s/Hz) are presented for comparison. As shown in Fig. 4, the proposed scheme with 3 layers and 16-QAM is still better than ACO-OFDM of 128-QAM with the same spectral efficiency.

The average BER performance for different layers with the same modulation order (16-QAM) and the performances of the original ACO-OFDM with 128-QAM is shown in Fig. 5. The performance degradation of the proposed scheme with 2 layers is 1dB at BER of  $10^{-3}$  compared with the conventional scheme. The performance degradation of the proposed scheme with 3 layers and 4 layers are 2dB and 3dB respectively at BER of  $10^{-3}$ . The LACO-OFDM spectral efficiencies with different layers of 2 layers, 3 layers and 4 layers are 1.5 bits/s/Hz, 1.75 bits/s/Hz and 1.875 bits/s/Hz respectively. The proposed scheme with 4 layers and 16QAM (1.875 bits/s/Hz) is also better than ACO-OFDM of 128-QAM with the spectral efficiency of 1.75 bits/s/Hz.



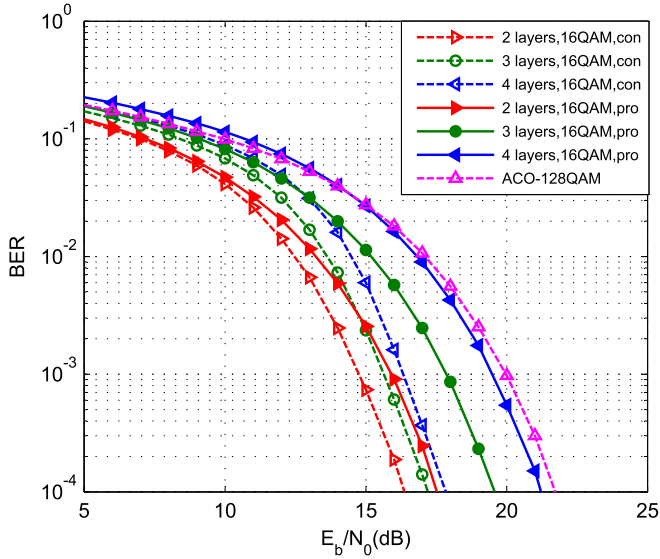


Fig. 5. BER performance comparison of the proposed and the conventional scheme with 16-QAM and different layers.

### B. LED Nonlinearity Channel

Experimental studies indicate that the LED nonlinearity is a major challenge for the OFDM-based VLC system [20–23]. The Rapps model is commonly utilized to describe the nonlinear behavior of power amplifier (PA), which is first employed for describing the LED nonlinearity [24]. The Rapps LED model can be given by

$$I_{\text{LED},n} = \begin{cases} \frac{f(x_{\text{L/EACO},n})}{(1+(f(x_{\text{L/EACO},n})/I_{\text{max}})^{2a})^{1/2a}}, & \text{if } x_{\text{L/EACO},n} \geq 0 \\ 0, & \text{if } x_{\text{L/EACO},n} < 0 \end{cases}, \quad (17)$$

where  $I_{\text{max}}$  is the maximum permissible current through the LED,  $a$  is the knee factor that is set to 2 in this section, and  $f(x_{\text{L/EACO},n}) = x_{\text{L/EACO},n}/R$ , where  $R$  is set to be a 1  $\Omega$  normalization resistance. The LED nonlinearity distorts the amplitude of OFDM signal and forces the lower peaks to be clipped [24]. This is similar to the clipping distortion for OFDM systems. Therefore, the nonlinearity level  $\beta$  is defined with similar definition of clipping level in [25]

$$\beta = 10 \log_{10} (I_{\text{max}}^2 / \sigma^2) \text{ dB}, \quad (18)$$

where  $\sigma^2$  is the power of  $x_{\text{L/EACO}}$ . The typical range of the nonlinearity for LACO-OFDM systems is from 5dB to 13dB [25]–[27].

The BER performance of LACO-OFDM with 3 layers in linear channel (lin) and LED nonlinearity channel ( $\beta = 9\text{dB}$ ) is presented in Fig. 6. In LACO-OFDM, Layer 1 has the most number of subcarriers with a high peak to average power ratio leading to the severe nonlinear distortion, which may result in the BER degradation [27]. In contrast, Layer 2 and Layer 3 have the less number of subcarriers respectively, which may lead to the lower nonlinear distortion as shown in Fig. 6(b), (c) and (d). However, this will have different results for the conventional scheme. Comparing Fig. 6(a) with Fig. 6(c) we can see that, the

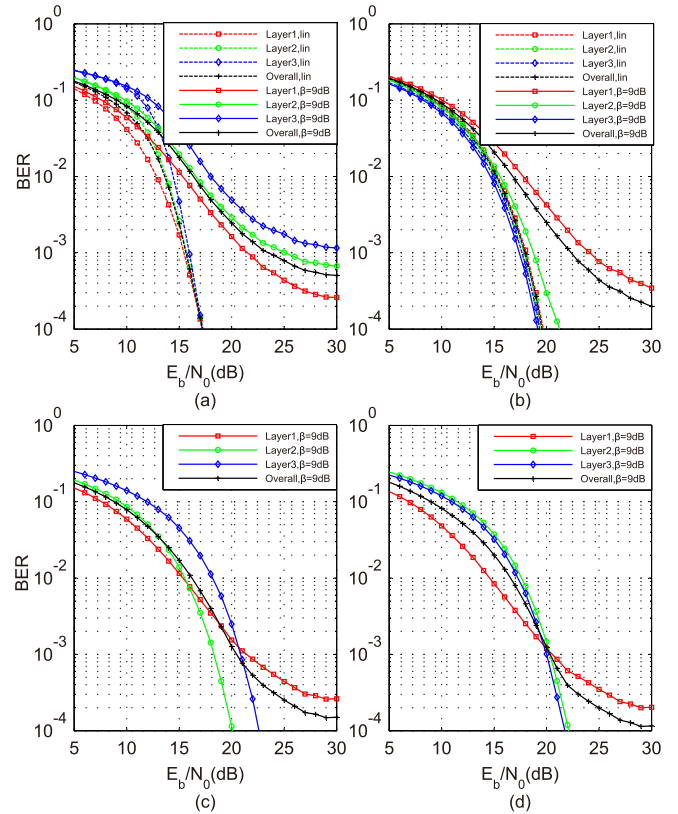


Fig. 6. BER performance of LACO-OFDM with 3 layers and 16-QAM in linear channel (lin) and LED nonlinearity channel ( $\beta = 9\text{dB}$ ): (a) the conventional scheme, (b) the proposed scheme, (c) the conventional scheme without the iterative detection, and (d) the proposed scheme with the optimized power.

nonlinear distortion in Layer 1 is introduced into higher layers by the iterative detection in the conventional scheme, which leads to the degradation of BER performance for Layer 2 and Layer 3. When the LED nonlinearity is considered in AWGN channel, the system performance depends not only on AWGN but also on nonlinear distortion. For the same BER level of  $10^{-3}$  for each layer, the power of subcarriers in Layer 2 ( $P_2$ ) is loaded by the allocation of  $P_2 = 0.51P_1$  and the subcarrier power allocation of Layer 3 is  $P_3 = 2P_2$  in Fig. 6(d). It is also shown that the same BER performance can be achieved for the proposed scheme and the conventional scheme without the iterative detection. It is noted that we have tried to set the optimized power for the conventional scheme, but it still doesn't work. It is found that when not all of layers are distorted severely by LED nonlinearity, the power adjustment can work.

Fig. 7 illustrates the BER performance of the proposed scheme and the conventional scheme using the Rapps LED model for different nonlinear levels, in which LACO-OFDM with 3 layers and 16-QAM is considered. In this case, when  $\beta$  is set to 10 dB, the proposed scheme has almost the same performance at the BER of  $10^{-3}$  compared to the conventional solution as shown in Fig. 7. When  $\beta$  is less than 10 dB, the performances of the proposed scheme outperform the conventional results. The proposed scheme is less sensitive to the LED nonlinearity, in which the nonlinear distortion in Layer 1 is not introduced into

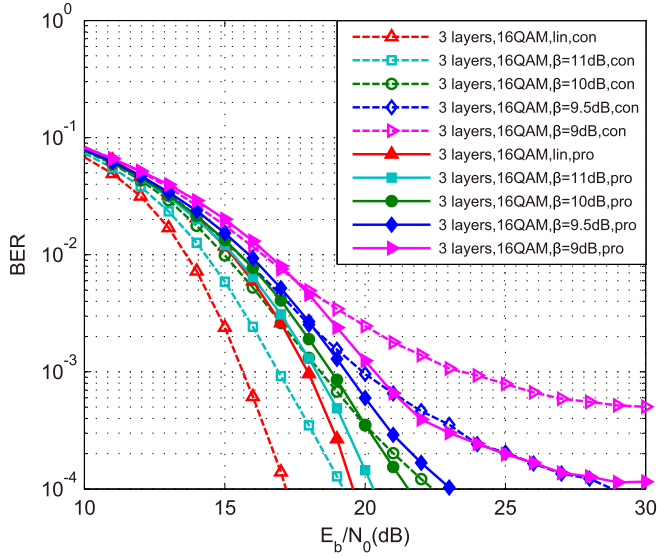


Fig. 7. BER performance comparison of the proposed scheme and the conventional scheme with 16-QAM and 3 layers for different nonlinear levels.

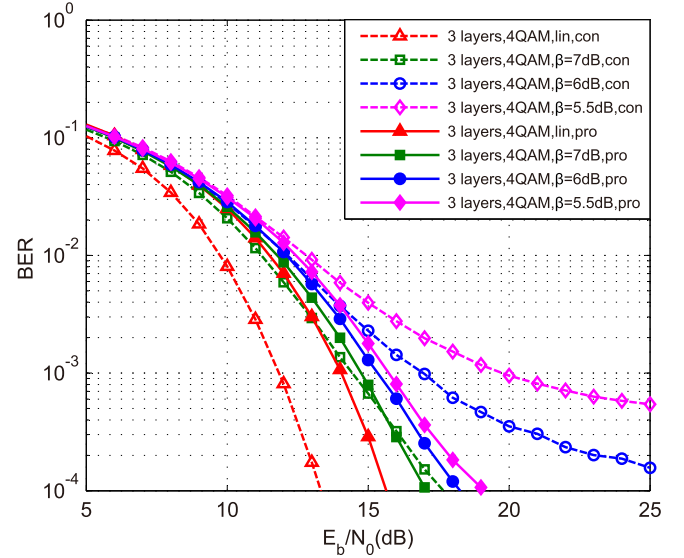


Fig. 8. BER performance comparison of the proposed scheme and the conventional scheme with 3 layers and 4-QAM for different nonlinear levels.

TABLE I  
LIST OF PARAMETERS FOR FIG. 7, FIG. 8, FIG. 9, FIG. 10 AND FIG. 11

Layers	$M$ -QAM	$\beta$	Power allocation for the proposed scheme
2	16-QAM	10.0 dB	$P_2 = 0.87P_1$
		9.5 dB	$P_2 = 0.68P_1$
		9.0 dB	$P_2 = 0.48P_1$
3	4-QAM	7.0 dB	$P_2 = 0.95P_1, P_3 = 2P_2$
		6.0 dB	$P_2 = 0.72P_1, P_3 = 2P_2$
		5.5 dB	$P_2 = 0.51P_1, P_3 = 2P_2$
	16-QAM	11.0 dB	$P_2 = 1.41P_1, P_3 = 2P_2$
		10.0 dB	$P_2 = 1.05P_1, P_3 = 2P_2$
		9.5 dB	$P_2 = 0.79P_1, P_3 = 2P_2$
64-QAM	9.0 dB	$P_2 = 0.51P_1, P_3 = 2P_2$	
	12.5 dB	$P_2 = 1.26P_1, P_3 = 2P_2$	
	11.8 dB	$P_2 = 0.87P_1, P_3 = 2P_2$	
4	16-QAM	11.3 dB	$P_2 = 0.51P_1, P_3 = 2P_2$
		10.0 dB	$P_2 = 1.25P_1, P_3 = 2P_2, P_4 = 4P_2$
		9.5 dB	$P_2 = 1.05P_1, P_3 = 2P_2, P_4 = 4P_2$
		9.0 dB	$P_2 = 0.66P_1, P_3 = 2P_2, P_4 = 4P_2$
		8.7 dB	$P_2 = 0.52P_1, P_3 = 2P_2, P_4 = 4P_2$

higher layers. However, in the conventional scheme, the more nonlinear distortion in Layer 1 is introduced into higher layers with the increasing of nonlinear distortion, which leads to a worse BER. For example, almost 3 dB gain can be achieved for the proposed scheme comparing with the conventional solution when  $\beta$  is reduced to 9 dB. The parameters of the subcarrier power in Layer  $l$  ( $P_l$ ) at the BER of  $10^{-3}$  are given in Table I.

The BER performance of LACO-OFDM with 3 layers and 4-QAM in LED nonlinearity channel is presented in Fig. 8. When  $\beta$  is set to 7 dB, the proposed scheme has almost the same BER at  $10^{-3}$  compared to the conventional solution. When  $\beta$  is reduced to 5.5 dB, almost 3 dB gain is also achieved compared with the conventional scheme.

Fig. 9 shows the BER performance of LACO-OFDM with 3 layers and 64-QAM in LED nonlinearity channel. When  $\beta$  is set to 11.8 dB, the proposed scheme has almost the same

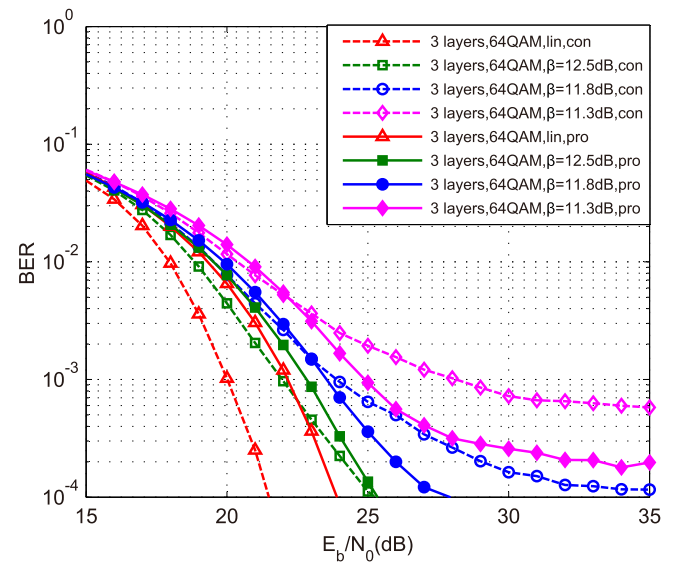


Fig. 9. BER performance comparison of the proposed scheme and the conventional scheme with 3 layers and 64-QAM for different nonlinear levels.

performance at the BER of  $10^{-3}$  compared to the conventional solution. The proposed scheme achieves almost 3 dB gain at the BER of  $10^{-3}$  compared with the conventional solution when  $\beta$  is set to 11.3 dB.

As shown in Fig. 10, when  $\beta$  is less than 10 dB, the proposed scheme with 2 layers and 16-QAM has the better performance than the conventional result at BER of  $10^{-3}$ . Fig. 11 shows that when  $\beta$  is less than 9.5 dB, the BER performance of the proposed scheme with 4 layers and 16-QAM still outperforms the conventional results. It is obvious that when the different layers or different QAM constellations are employed for LACO-OFDM, the proposed scheme has the better performance than that of the conventional scheme in the high nonlinearity channel.

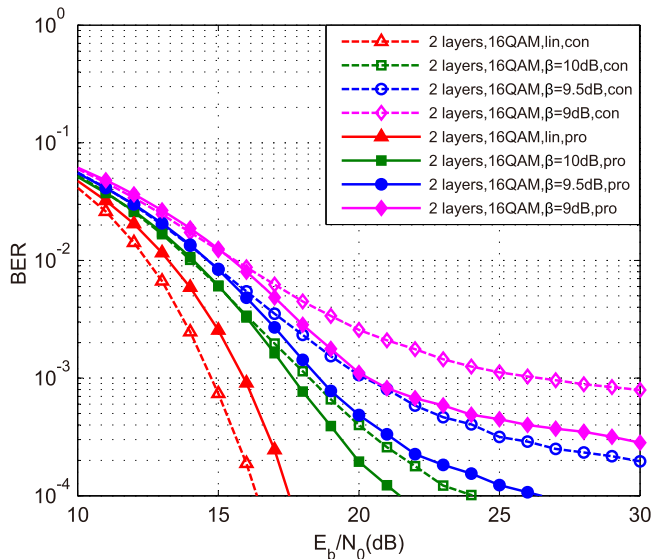


Fig. 10. BER performance comparison of the proposed scheme and the conventional scheme with 2 layers and 16-QAM for different nonlinear levels.

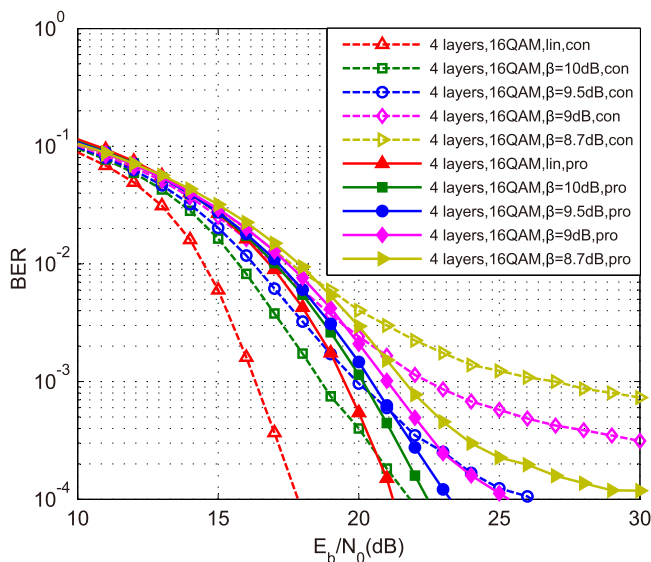


Fig. 11. BER performance comparison of the proposed scheme and the conventional scheme with 4 layers and 16-QAM for different nonlinear levels.

Therefore, the single-FFT receiver shows its advantages in LED nonlinearity channel for LACO-OFDM based VLC systems.

#### IV. CONCLUSION

In this paper, a low complexity receiver using a single FFT is proposed for LACO-OFDM based VLC systems. In the conventional LACO-OFDM receiver, the different layers of ACO-OFDM signals are distinguished in frequency domain by a FFT/IFFT pair which may lead to an increased complexity for the receiver. However, the proposed receiver does not require the FFT/IFFT pair, which makes it relatively simple, and the complexity of  $O(N \log_2 N)$  can be achieved. Simulation

results illustrate that the proposed scheme has a SNR penalty of 1dB  $\sim$  3dB at the BER of  $10^{-3}$  compared with the conventional solution in the AWGN channel. Furthermore, simulation results show that the proposed scheme has the better performance than the conventional solution in LED nonlinearity channel. The single-FFT receiver will be a good candidate for the LACO-OFDM system which is affected by LED nonlinearity or requires the low complexity.

#### REFERENCES

- [1] H. Elgala, R. Mesleh, and H. Haas, "Indoor optical wireless communication: Potential and state-of-the-art," *IEEE Commun. Mag.*, vol. 49, no. 9, pp. 56–62, Sep. 2011.
- [2] A. Jovicic, J. Li, and T. Richardson, "Visible light communication: opportunities, challenges and the path to market," *IEEE Commun. Mag.*, vol. 51, no. 12, pp. 26–32, Dec. 2013.
- [3] D. Tsonev *et al.*, "A 3-Gb/s single-LED OFDM-based wireless VLC link using a gallium nitride  $\mu$ LED," *IEEE Photon. Technol. Lett.*, vol. 26, no. 7, pp. 637–640, Jan. 2014.
- [4] D. Tsonev, S. Videv, and H. Haas, "Towards a 100 Gb/s visible light wireless access network," *Opt. Express*, vol. 23, no. 2, pp. 1627–1637, Jan. 2015.
- [5] J. Armstrong and A. J. Lowery, "Power efficient optical OFDM," *Electron. Lett.*, vol. 42, no. 6, pp. 370–372, Mar. 2006.
- [6] S. D. Dissanayake and J. Armstrong, "Comparison of ACO-OFDM, DCO-OFDM and ADO-OFDM in IM/DD systems" *J. Lightwave Technol.*, vol. 31, no. 7, pp. 1063–1072, Jan. 2013.
- [7] B. Ranjha and M. Kavehrad, "Hybrid asymmetrically clipped OFDM-based IM/DD optical wireless system," *J. Opt. Commun. Netw.*, vol. 6, no. 4, pp. 387–396, May 2014.
- [8] H. Elgala and T. D. C. Little, "SEE-OFDM: Spectral and energy efficient OFDM for optical IM/DD systems," in *Proc. IEEE 25th Annu. Int. Symp. Pers. Indoor, Mob. Radio Commun.*, 2014, pp. 851–855.
- [9] D. Tsonev, S. Videv, and H. Haas, "Unlocking spectral efficiency in intensity modulation and direct detection systems," *IEEE J. Sel. Areas Commun.*, vol. 33, no. 9, pp. 1758–1770, May 2015.
- [10] M. S. Islam, D. Tsonev, and H. Haas, "On the superposition modulation for OFDM-based optical wireless communication," in *Proc. IEEE Glob. Conf. Signal Inf. Process.*, 2015, pp. 1022–1026.
- [11] M. S. Islam and H. Haas, "Augmenting the spectral efficiency of enhanced PAM-DMT-based optical wireless communications," *Opt. Express*, vol. 24, no. 11, pp. 11932–11949, May 2016.
- [12] Q. Wang, C. Qian, X. Guo, Z. Wang, D. G. Cunningham, and I. H. White, "Layered ACO-OFDM for intensity-modulated direct-detection optical wireless transmission," *Opt. Express*, vol. 23, no. 9, pp. 12382–12393, May 2015.
- [13] A. J. Lowery, "Comparisons of spectrally-enhanced asymmetrically clipped optical OFDM systems," *Opt. Express*, vol. 24, no. 4, pp. 3950–3966, Feb. 2016.
- [14] Q. Wang, Z. Wang, X. Guo, and L. Dai, "Improved receiver design for layered ACO-OFDM in optical wireless communications," *IEEE Photon. Technol. Lett.*, vol. 28, no. 3, pp. 319–322, Feb. 2016.
- [15] M. M. A. Mohammed, C. He, and J. Armstrong, "Diversity combining in layered asymmetrically clipped optical OFDM," *J. Lightwave Technol.*, vol. 35, no. 11, pp. 2078–2085, Jun. 2017.
- [16] T. H. Wang, H. Li, and X. Huang, "Interference cancellation for layered asymmetrically clipped optical OFDM with application to optical receiver design," *J. Lightwave Technol.*, vol. 36, no. 11, pp. 2100–2113, Jun. 2018.
- [17] Q. Wang *et al.*, "Hardware-efficient signal generation of layered/enhanced ACO-OFDM for short-haul fiber-optic links," *Opt. Express*, vol. 25, no. 12, pp. 13359–13371, Jun. 2017.
- [18] J. Li, X. Liu, J. Li, and Z. Huang, "Diversity combining via symmetry recovering for asymmetrically clipped optical OFDM," *Opt. Commun.*, vol. 443, pp. 86–89, Mar. 2019.
- [19] J. Vucic, C. Kottke, S. Nerretter, K. D. Langer, and J. W. Walewski, "513Mbit/s visible light communications link based on DMT-modulation of a white LED," *J. Lightwave Technol.*, vol. 28, no. 24, pp. 3512–3518, Oct. 2010.
- [20] J. Li, Z. Huang, X. Liu, and Y. Ji, "Hybrid time-frequency domain equalization for LED nonlinearity mitigation in OFDM-based VLC systems," *Opt. Express*, vol. 23, no. 1, pp. 611–619, Jan. 2015.

- [21] I. Neokosmidis, T. Kamalakis, J. W. Walewski, B. Inan, and T. Spicopoulos, "Impact of nonlinear LED transfer function on discrete multitone modulation: Analytical approach," *J. Lightw. Technol.*, vol. 27, no. 22, pp. 4970–4978, Nov. 2009.
- [22] G. Stepniak, J. Siuzdak, and P. Zwierko, "Compensation of a VLC phosphorescent white LED nonlinearity by means of Volterra DFE," *IEEE Photon. Technol. Lett.*, vol. 25, no. 16, pp. 1597–1600, Aug. 2013.
- [23] G. Zhang, J. Zhang, X. Hong, and S. He, "Low-complexity frequency domain nonlinear compensation for OFDM based high-speed visible light communication systems with light emitting diodes," *Opt. Express*, vol. 25, no. 4, pp. 3780–3794, Feb. 2017.
- [24] H. Elgala, R. Mesleh, and H. Haas, "An LED model for intensity-modulated optical communication systems," *IEEE Photon. Technol. Lett.*, vol. 22, no. 11, pp. 835–837, Apr. 2010.
- [25] R. Bai, Z. Wang, R. Jing, and J. Cheng, "Interleaved DFT-spread layered/enhanced ACO-OFDM for intensity-modulated direct-detection systems," *J. Lightwave Technol.*, vol. 36, no. 20, pp. 4713–4722, Oct. 2018.
- [26] X. Zhang, Q. Wang, R. Zhang, S. Chen, and L. Hanzo, "Performance analysis of layered ACO-OFDM," *IEEE Access*, vol. 5, pp. 18366–18381, Aug. 2018.
- [27] T. Q. Wang, H. Li, and X. Huang, "Analysis and mitigation of clipping noise in layered ACO-OFDM based visible light communication systems," *IEEE Trans. Commun.*, vol. 67, no. 1, pp. 564–577, Sep. 2019.

**Xiaoshuang Liu** received the B. S. and M. S. degrees in mathematics and applied mathematics from Hebei Normal University, Hebei, China, in 2009 and 2012, respectively and the Ph.D. in information and communication engineering from Beijing University of Posts and Telecommunications Beijing, China, in 2015. She is currently a Lecturer with the School of Information Technology, Hebei University of Economics and Business, Hebei, China. Her research interests include orthogonal frequency division multiplexing and visible light communications.

**Jianfeng Li** received the B.E. and M.E. degrees in optical engineering from the Yanshan University, Hebei, China, in 2009 and 2012 respectively, and the Ph.D. degree in information and communication engineering from Beijing University of Posts and Telecommunications Beijing, China, in 2015. He is currently a Lecturer with the School of Information Technology, Hebei University of Economics and Business, Hebei, China. His research interests include visible light communications, orthogonal frequency division multiplexing, modulation, and LED nonlinearity.

**Jianke Li** received the B.E. degree in electronic engineering from the Hebei Institute of Mechanical and Electronic Technology, Hebei, China, in 1994 and the M.E. degree in electronic engineering from the Yanshan University, Hebei, China, in 2005 and the Ph.D. degree in electronic engineering from Beijing Institute of Technology, Beijing, China, in 2011. He is currently a Professor with the School of Information Technology, Hebei University of Economics and Business, Hebei, China. His research interests include signal processing, and deep learning.

**Zhitong Huang** received the B.E. and Ph.D. degrees in information and communication engineering from Beijing University of Posts and Telecommunications Beijing, China, in 2003 and 2008, respectively. He is currently a Professor with the State Key Laboratory of Information Photonics and Optical Communications, Beijing University of Posts and Telecommunications, Beijing, China. His research interests include visible light communications, orthogonal frequency division multiplexing, and optical wireless networks.